Mechanisms of damage to corals exposed to sedimentation

Miriam Weber[a,b,c,1], Dirk de Beer[a], Christian Lott[a,b], Lubos Polerecky[a], Katharina Kohls[a], Raeid M. M. Abed[d], Timothy G. Ferdelman[a], and Katharina E. Fabricius[c]

[a]Max Planck Institute for Marine Microbiology, 28359 Bremen, Germany; [b]HYDRA Institute for Marine Sciences, Elba Field Station, 57034 Campo nell'Elba, Italy; [c]Australian Institute of Marine Science, Townsville, Queensland 4810, Australia; and [d]Biology Department, College of Science, Sultan Qaboos University, Muscat 123, Sultanate of Oman

Edited by Thomas J. Goreau, Global Coral Reef Alliance, Cambridge, MA, and accepted by the Editorial Board March 12, 2012 (received for review January 19, 2011)

We investigated the mechanisms leading to rapid death of corals when exposed to runoff and resuspended sediments, postulating that the killing was microbially mediated. Microsensor measurements were conducted in mesocosm experiments and in naturally accumulated sediment on corals. In organic-rich, but not in organic-poor sediment, pH and oxygen started to decrease as soon as the sediment accumulated on the coral. Organic-rich sediments caused tissue degradation within 1 d, whereas organic-poor sediments had no effect after 6 d. In the harmful organic-rich sediment, hydrogen sulfide concentrations were low initially but increased progressively because of the degradation of coral mucus and dead tissue. Dark incubations of corals showed that separate exposures to darkness, anoxia, and low pH did not cause mortality within 4 d. However, the combination of anoxia and low pH led to colony death within 24 h. When hydrogen sulfide was added after 12 h of anoxia and low pH, colonies died after an additional 3 h. We suggest that sedimentation kills corals through microbial processes triggered by the organic matter in the sediments, namely respiration and presumably fermentation and desulfurylation of products from tissue degradation. First, increased microbial respiration results in reduced O_2 and pH, initiating tissue degradation. Subsequently, the hydrogen sulfide formed by bacterial decomposition of coral tissue and mucus diffuses to the neighboring tissues, accelerating the spread of colony mortality. Our data suggest that the organic enrichment of coastal sediments is a key process in the degradation of coral reefs exposed to terrestrial runoff.

microbial activity | acidification | fertilizer input | urbanization | coastal management

Worldwide, coastal coral reefs are threatened by eutrophication and sedimentation from terrestrial runoff (1, 2). Sedimentation events after terrestrial runoff or wave resuspension expose corals to fine nutrient-rich sediment that, when settled on reef-building corals, can bleach or kill exposed tissues (3). The extent of photophysiological stress in corals correlates with the amount of sedimentation multiplied by exposure time (4). Few coral communities are adapted to muddy sediment (5), and the negative impacts on the coral holobiont (the animal and its algal symbionts) of enhanced sedimentation on corals are widely documented (reviewed in refs. 6 and 7). However, earlier studies either did not characterize the sediments or regarded them mainly as mineral particles (8–10), and the microbial and chemical components have not been analyzed. Therefore the mechanisms leading to coral mortality after sediment exposure still are poorly understood.

Sediments carry adsorbed or particulate nutrients and contaminants (11) and contain varying proportions of organic particles such as fecal pellets, detritus, and exopolymeric substances (12). Sediments mostly form aggregates harboring phytoplankton (13) and highly active microbial communities (14, 15). Earlier studies contrasting the effects of sedimentation with varying sediment properties showed that estuarine silt enriched with marine snow smothered and killed coral juveniles and reef organisms within hours to days, whereas silt without enrichment was rejected by the organisms (16, 17). Another study showed the important role of sediment grain size and biogeochemical properties. Fine sediments rich in organic matter led to coral death within 1 or 2 d, whereas coarse sediments and fine sediments poor in organic matter did not damage the corals (3). Kline et al. (18) showed that increased concentrations of dissolved organic carbon in the experiment tank water led to increased growth rates of the microbes in the coral's surface mucus layer, leading to coral mortality. In 1990 Hodgson (19) postulated that sediment is not harmful per se but becomes harmful when microbes are present in the sediment, because the presence of tetracycline reduced coral mortality caused by sedimentation. These findings suggest that enhanced microbial growth favored by elevated organic matter content could be fatal for corals covered with organic-rich sediment.

The motivation for this study was to understand better the mechanisms underlying sediment-induced coral mortality. Some studies suggested that coral damage might be caused by the absence of light under the sediment, leading to the inhibition of the photosynthesis of the zooxanthellae and eventually to anoxia (4, 8), finally breaking down the living holobiont by expulsion or loss of its algal partner. Others suggested that hydrogen sulfide (H_2S), known for its toxicity to many life forms (20), is the main causative agent for coral damage (3). Sulfate reduction is the prevailing microbial process in anoxic sediments (21) and leads to the formation of H_2S. Previous work concluded that sulfate reduction enhanced by eutrophication in sediments might kill corals in their vicinity (22, 23). In studies on the coral black band disease it was proposed that the microbial community causing the disease contributes to tissue lysis by the production of H_2S (24, 25).

The goal of this study was to demonstrate the mechanism of rapid coral mortality induced by exposure to organic-rich sedimentation, postulating that the process is mediated by microbial activity in the sediment. We tested the hypothesis that sulfide formed by sedimentary sulfate reduction kills the sediment-covered coral. The study is based on three controlled laboratory experiments and on experiments conducted with naturally accumulated sediment layers on corals on inshore and offshore coral reefs. In the laboratory experiments, we chose natural plankton,

Author contributions: M.W., D.d.B., C.L., and K.E.F. designed research; M.W. and C.L. performed research; D.d.B., K.K., R.M.M.A., T.G.F., and K.E.F. contributed new reagents/analytic tools; M.W., L.P., and K.E.F. analyzed data; and M.W., D.d.B., C.L., L.P., K.K., and K.E.F. wrote the paper.

The authors declare no conflict of interest.

This article is a PNAS Direct Submission. T.J.G. is a guest editor invited by the Editorial Board.

Freely available online through the PNAS open access option.

[1]To whom correspondence should be addressed. E-mail: m.weber@hydra-institute.com.

See Author Summary on page 9242 (volume 109, number 24).

This article contains supporting information online at www.pnas.org/lookup/suppl/doi:10.1073/pnas.1100715109/-/DCSupplemental.

which was added to the sediments at environmentally relevant concentrations, as our source of organic carbon. We used microsensors, radioisotopes, molecular tools, and modeling. The effects of putative damaging factors, namely darkness, anoxia, lowered pH, and H_2S, were tested separately and in combination. From these experiments we deduced the possible succession of processes that is responsible for coral death caused by sedimentation.

Results

First, the results of the measurements and observations in the sediment layer and of the corals are presented in a summary to illustrate the iterative approach and the rationale of the experiments. We then describe each experiment in detail (Figs. 1–7 and Tables 1–4).

After 1 d of exposure to a layer of sediment with a thickness of 2–2.5 mm and an enrichment of +0.6% organic carbon (C_{org}), the first spots of degraded coral tissue were detected (Figs. 1 and 2*A*). At this point in time we measured anoxia, pH 7.1, and a concentration of 1–2 μM of H_2S at the coral–sediment interface (Fig. 3). To differentiate the possible sources of total sulfide (S_{tot}), we compared the S_{tot} concentrations calculated from the sulfate reduction rates (SRRs) in the sediment with the data from the microsensor measurements (Table 1). The calculated concentration of S_{tot} at the coral surface produced by sulfate reduction after 1 d (0.22 μM S_{tot}) was one order of magnitude lower than the real concentrations measured with the microsensors (2.2 μM S_{tot}) (Fig. 4*B*). This comparison revealed that 90% of the measured H_2S was the product of another process, presumably desulfurylation of dead coral tissue (Table 1). That finding would mean that the coral was degraded before sulfate reduction within the sediment led to lethal H_2S concentrations and that the initial coral degradation must have been caused by factors other than H_2S. The chronology of H_2S development also shows that the onset of massive sulfide production occurred after the death of the coral: In experiment 1 we measured an increase in H_2S from 1–2 μM (anoxia, pH 7.1) after 24 h to 50 μM H_2S (anoxia, pH 7.4) after 48 h, to 107.5 μM H_2S (anoxia, pH 6.9) after 72 h, and to 122.1 μM H_2S (anoxia, pH 6.9) after 96 h (Fig. 3) at the sediment–coral interface. Profiles through the entire sediment layer are displayed in *SI Appendix*, Fig. S1.

To find out whether H_2S is needed to kill the corals within 1 d, we exposed corals without using sediment to the conditions we had measured with the microsensors in the sediment layer. In the exposure experiment corals kept under anoxia and pH 7 were dead within 1 d without the addition of H_2S. We also tested the cumulative effect of anoxia, pH, and sulfide on the corals (experiment 3). First the corals were kept under anoxia and pH 7 for 12 h, at which point the corals were still alive; then we added 20 μM H_2S and left the coral in the tank for another 3 h. The coral did not survive this combined treatment after a total of 15 h (Tables 2–4); in this case H_2S in combination with anoxia and lowered pH accelerated the processes leading to coral death, but H_2S was not a prime cause of death.

Experiment 1: Sediment Exposure in Mesocosms. The photosynthetic yield (i.e., the quantum yield of photochemical energy conversion) of control corals remained similar from the beginning to the end of experiment 1 (0.656 ± 0.052 vs. 0.652 ± 0.049). The control corals therefore did not show photophysiological stress. Photosynthetic yields in corals exposed to sediments with +0 and +0.06% C_{org} also did not change during the experiment (Fig. 2*B*). In contrast, corals exposed to sediment with +0.3 and +0.6% C_{org} showed a continuous decrease in photosynthetic yields, and coral tissue degradation occurred. Tissue degradation of a few square millimeters was observed first after 1 d in the +0.6% C_{org} treatment (Figs. 1 and 2*A*). The decline in photosynthetic quantum yields and increasing tissue degradation correlated with the amount of C_{org} enrichment and exposure time (Fig. 2). Results of generalized linear models, with estimates indicating the differences between treatments, are shown in *SI Appendix*, Table S1.

All sediment covers strongly attenuated light: Light decreased exponentially, reaching 43, 9, and <1% of the surface level at sediment depths of 0.5, 1, and 1.5 mm, respectively. The decrease of O_2 concentrations and pH in the sediment layer covering the coral correlated significantly with increasing C_{org} concentration (Fig. 3 and *SI Appendix*, Fig. S1 and Table S1). Sediments with concentrations of +0 and +0.06% C_{org} were suboxic but never anoxic, and the pH at the coral surface remained around 8.0–8.1 (Fig. 3). Exposure to sediments enriched with +0.3 and +0.6% C_{org} caused anoxia at the coral surface after only 3 h. The pH on

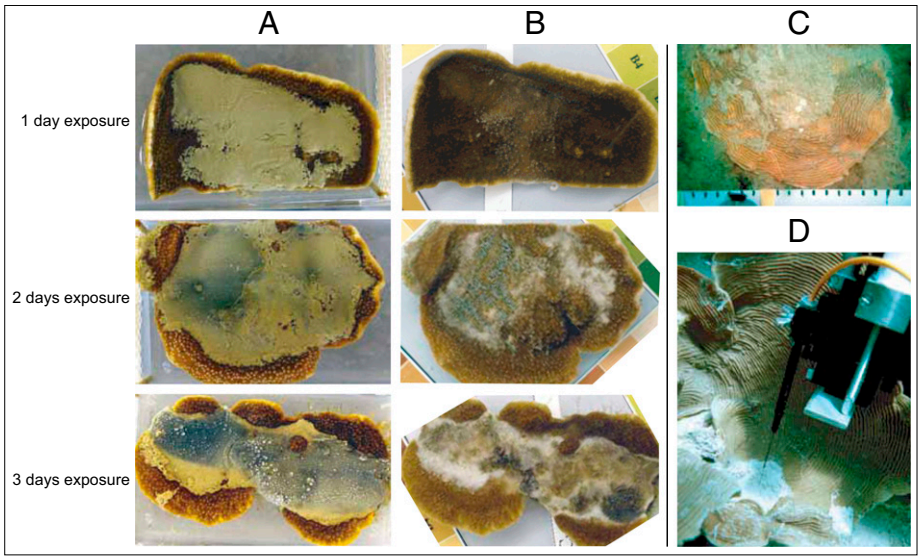

Fig. 1. (*A* and *B*) Fragments of the coral *M. peltiformis* covered with sediment that was enriched with +0.6% C_{org} (*A*) and the same coral fragments after the sediment was removed (*B*). Exposure times were 1, 2, and 3 d; areas of degraded tissue were detected first after 1 d. The sediments covering the corals became colonized by white sulfur-oxidizing bacteria from day 2 onwards, and colonies were clearly visible at day 3. (*C* and *D*) Underwater images of two corals with naturally accumulated sediment at a nearshore (*C*) and an offshore reef (*D*).

Table 1. Concentrations and fluxes of total sulfide (S_{tot}) at the sediment and coral surface, derived from microsensor measurements and from a model

	Sediment surface		Coral surface		Sediment
Time	S_{tot} (mmol m^{-3})	S_{tot} flux (nmol m^{-2} s^{-1})	S_{tot} (mmol m^{-3})	J_d (nmol m^{-2} s^{-1})	SRR_a (nmol m^{-2} s^{-1})
24 h					
Measured	0	−2.2	2.2	—	0.36
Scenario A	0.02	−0.36	0.22	0	0.36
Scenario B	0.11	−2.08	2.2	−1.72	0.36
48 h					
Measured	110	−290	370	—	1.6
Scenario A	0.26	−1.6	1.15	0	1.6
Scenario B	50	−305	384	−303	1.6

Measurements were conducted as described in the experiments 1 and 2. In the model scenario A, S_{tot} was produced exclusively by sulfate reduction in the sediment covering the coral. The areal rate of this process (SRR_a) was calculated by multiplying the measured volumetric SRR (Fig. 5) with the thickness of the sediment layer covering the coral. In the model scenario B, coral tissue decomposition contributed to S_{tot}. The total sulfide flux due to coral tissue decomposition, J_d, was adjusted in the model to match the measured and calculated profiles.

the coral surface covered with +0.3 and +0.6% C_{org} sediments decreased to 6.6 ± 0.15 and 6.9 ± 0.3, respectively (Fig. 3 and *SI Appendix*, Table S1). The increase of H_2S concentrations correlated with increasing exposure time together with C_{org} concentration at the coral surface (Fig. 3 and *SI Appendix*, Table S1). No H_2S was measured in the +0 and +0.06% C_{org} sediments. Concentrations of the H_2S at the coral surface under the sediment enriched with +0.3% reached 1–2 ± 1 μM after 48 h, and concentrations of H_2S under the sediment enriched with +0.6% C_{org} reached 1–2 ± 1 μM after only 24 h exposure. After another 24 h, H_2S concentrations increased by two orders of magnitude. The microsensor profiles of concentrations of O_2, S_{tot}, H_2S, and pH in the sediment layer on the coral are shown in *SI Appendix*, Fig. S1.

In the field, light, O_2, and pH profiles also were measured on corals naturally covered with sediment. The thickness of the sediment layer covering corals in the field varied between 2 and 2.5 mm. Light intensity had decreased to <1% of ambient light in all samples at a sediment depth of 1.5 mm (Fig. 6). No detectable light (<0.1 μmol photons · m^{-2} · s^{-1}) reached the coral surface. At the offshore sites O_2 concentrations were reduced, but none of the O_2 profiles showed anoxia (minimum: 10 μM O_2) at the coral surface under the sediment layer (Fig. 6). At the nearshore sites O_2 was depleted completely under the sediment layer in three of four corals, and the corals experienced anoxic conditions. In the anoxic sediment the pH was reduced to 7.6–7.7 ± 0.02 at the coral surface (Fig. 6). ANOVAs revealed that differences in the concentrations of total phosphorous (TP) and trace elements in the sediment layer deposited on coral colonies at inshore reefs were significantly higher than in sediment on corals at the offshore reefs. However, the content of chlorophyll a (Chl *a*), phaeophytin (Phaeo), total nitrogen (TN), total organic carbon (TOC), and the grain size distribution were not significantly different (*SI Appendix*, Table S3).

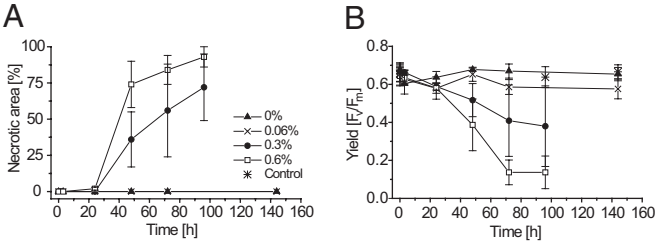

Fig. 2. The effects of sediment coverage on the coral *M. peltiformis* were recorded as (*A*) the percentage of degraded coral tissue on the sediment-covered area and (*B*) photosynthetic yields. In this mesocosm experiment the fine reef sediment was enriched with organic matter at four levels: +0, +0.06, +0.3, and +0.6% C_{org}. Error bars represent the SD (n = 4). For the statistical analysis see *SI Appendix*, Table S1.

In the mesocosm experiment 1, TOC, TN, TP, Chl *a*, and Phaeo increased over time in the +0.3- and +0.6% C_{org}-enriched sediment covering the corals but did not increase in the Petri dishes (*SI Appendix*, Fig. S2). Results of generalized linear models are given in *SI Appendix*, Table S4. The increases probably were caused by the death of the corals and subsequent release of these compounds from the decaying coral tissue under the sediment layer. Sediments with lower C_{org} (in which corals survived) and control sediments did not show changes in TOC, TN, and TP, but Chl *a* and Phaeo increased, likely because of microphytobenthos growth (*SI Appendix*, Fig. S2).

The structure of the bacterial community within the sediments of the mesocosm experiment 1 was investigated using denaturing gradient gel electrophoresis (DGGE) and 16S rRNA cloning. The DGGE banding patterns were similar in the control sediment and the sediments on the corals, suggesting that the structure of the microbial community of the sediment was independent of the presence of the underlying corals or coral mucus (Fig. 7). The dominant bacterial groups detected by DGGE analysis were *Bacteroidetes,* α- and γ-*Proteobacteria,* and *Fusobacteria* (Fig. 7). The comparative 16S rRNA sequence analysis showed that most sequences were related to the bacterial groups *Bacteroidetes,* α-, δ-, ε-, and γ-*Proteobacteria, Firmicutes,* and *Fusobacteria* (Fig. 7). Changes in the community diversity after 3 h and after 2, 4, and 6 d of exposure occurred in enriched and nonenriched sediments. The banding pattern of the +0% C_{org} sample is not very visible in the figure because the bands were very thin and weak; however, it followed the same pattern as the other treatments. The diversity was lowest in the sediment with the highest enrichment (+0.6% C_{org}) exposed for 3 h on the coral (Fig. 7; clone library C). This result suggests that the bacterial community reacts quickly to the enrichment of organic matter in the sediment, and a few bacterial groups become dominant. At the end of experiment 1 the microbial community of the enriched sediments returned to a diversity [Shannon–Wiener (SW) index of 3.3–3.47 in the clone library B, E, and F] similar to that of the stock sediment (clone library A, SW index 3.59). The community of the nonenriched sediment (clone library D) showed the highest diversity with an SW index of 4.26 (*SI Appendix*, Table S5). However, clone libraries should be compared cautiously, because there was only one library per treatment.

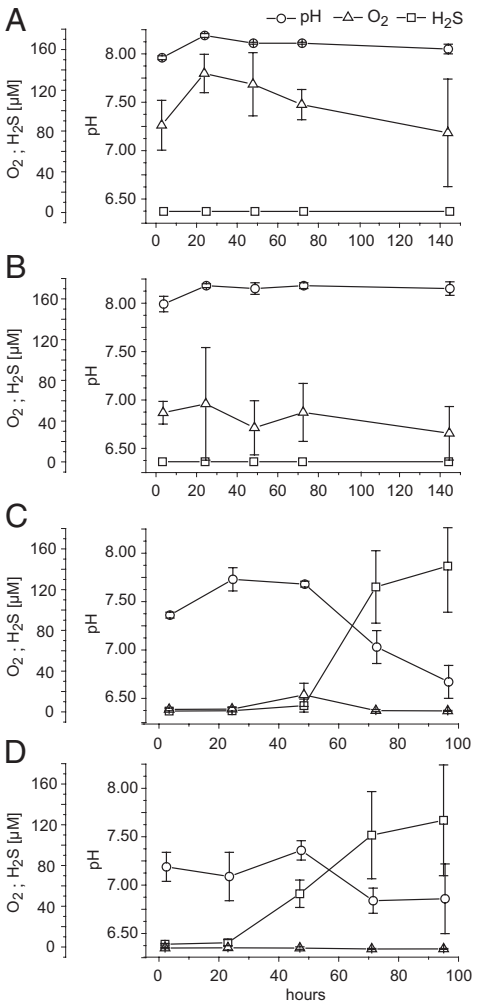

Fig. 3. In this mesocosm experiment the fine reef sediment was enriched with organic matter at four levels: +0 (*A*), +0.06 (*B*), +0.3 (*C*), and +0.6% C_{org} (*D*). The graphs show the concentration of O_2, pH, and H_2S at the coral–sediment interface of the coral *M. peltiformis* covered with sediment. Exposure times were 3 h or 1, 2, 3, and 4 or 6 d. Error bars represent the SD (n = 3–6). For the statistical analysis see the *SI Appendix*, Table S1.

Details on the 16S rRNA clone libraries are given in *SI Appendix*, Table S5.

Experiment 2: SRRs. The SRR in sediments not enriched with C_{org} remained low (<1 nmol·cm^{-3}·d^{-1}) even after the sediment had covered the corals for 2 d (Fig. 5). In contrast, the SRR of 0.6% C_{org}-enriched sediment increased over 2 d to 69.37 ± 11.73 nmol·cm^{-3}·d^{-1}. During the first 24 h the rate in the sediment on the corals was low (15.37 ± 2.26 nmol·cm^{-3}·d^{-1}) compared with the rate in the control sediment in the Petri dishes (62.14 ± 0.32 nmol·cm^{-3}·d^{-1}).

The S_{tot} profiles, derived from the measured H_2S and pH profiles, were almost linear within the sediment layer covering the coral (*SI Appendix*, Fig. S1). This result implies that the S_{tot} production by sulfate reduction in the sediment was negligible and that almost all sulfide originated from the coral surface, supposedly as a product of coral tissue decay by desulfurylation. This conclusion was supported by the model, which showed that the shape of the measured profiles could not be explained by assuming sulfate reduction in the sediment as the only source of sulfide. The S_{tot} concentrations on the top and at the bottom of the sediment layer, as well as the S_{tot} flux at the sediment surface, calculated from the measured SRRs (Fig. 5) using Eq. 3 and the total sulfide flux due to coral tissue decomposition J_d = 0 (*SI Appendix*, Table S6), were at least one order of magnitude lower than those measured with microsensors (Fig. 4 and Table 1, model scenario A). The measured and modeled profiles could be matched only by considering an additional source of sulfide at the sediment–coral interface. The flux of this additional sulfide source, J_d, ranged from about 1.7 nmol·m^{-2}·s^{-1} after 24 h to about 300 nmol·m^{-2}·s^{-1} after 48 h, 5- and 191-fold larger, respectively, than the depth-integrated SRR in the sediment covering the coral (Table 1, model scenario B). Thus the sulfate reduction in the sediment layer could not explain the measured H_2S concentrations and observed S_{tot} flux, and the H_2S must originate largely from below, e.g., from coral tissue decay by desulfurylation.

Experiment 3: Exposure to Anoxia, Reduced pH, and H_2S. The corals exposed in the dark to oxygenated water at pH 8.2 or 7.0 maintained high photosynthetic yields, as measured by pulse-amplitude modulated chlorophyll fluorometery (PAM) (Tables 2–4). The corals also survived for 4 d with similar photosynthetic yields under anoxic conditions at pH 8.2. However, simultaneous exposure to anoxia and reduced pH resulted in low photosynthetic yields after 24 h of exposure, and recovery was not successful. The photosynthetic yields decreased with time when corals were exposed to anoxia plus pH 7.0 or to anoxia plus pH 7.0 plus 10 µM H_2S. Recovery also failed when the corals were exposed to 10 and 20 µM H_2S at pH 7.0 and anoxia for 24 h. It is important to note that under these conditions the corals did not die when exposed to H_2S for 6 or 12 h (<24 h). In contrast, coral death occurred within 15 h when they first were exposed to anoxia at pH 7.0 for 12 h and then also were exposed to 20 µM sulfide for 3 h. This result suggests that the combination of anoxia and low pH kills corals, and H_2S further accelerates the die-off (Tables 2–4). Results of a generalized linear model are shown in *SI Appendix*, Table S7.

Discussion

River loads of nutrients from fertilizers, sewage, and eroding soils have increased globally since preindustrial times, affecting about 25% of coral reefs around the world (1). Anthropogenic fluxes of nitrogen and phosphorus from rivers into inshore coastal waters are considered to be two to three times higher now than before the industrial and agricultural revolutions (2). For the Great Barrier Reef, river exports of suspended sediments, TN, and TP have increased six- to ninefold since colonization (26), with much of the discharged material being retained on the wide and shallow continental shelf. The increased nutrient discharges lead to the organic enrichment of inshore sediments and a wide range of profound changes in the ecology of inshore coral reefs (7).

This study presents evidence that the mortality of corals exposed to sediments with increased concentrations of organic matter is microbially mediated, although by a different mechanism than expected. We provide evidence that the organic matter in the sediment leads to microbially induced anoxia and reduced pH, which causes coral death within 15–48 h, depending on the concentration of organic matter in the sediments. We observed that H_2S originating from sulfate reduction was not needed to kill the corals that were covered with sediment enriched with organic matter.

Sediments that are enriched in organic matter commonly settle and cover reef organisms after flood plumes and resuspension events, especially in areas exposed to coastal development (27, 28). Such sediments largely consist of labile high- and low-molecular-weight organic compounds (29), similar to the fresh plankton mixture we added. Fresh plankton, also including microbes, is known to release dissolved organic compounds that are extremely bioreactive (30) and immediately enhance microbial activity (31). Hydrolyzing, fermenting, and respiring bacteria, such as *Gammaproteobacteria*, *Bacteroidetes*, and *Fusobacteria*, respond quickly

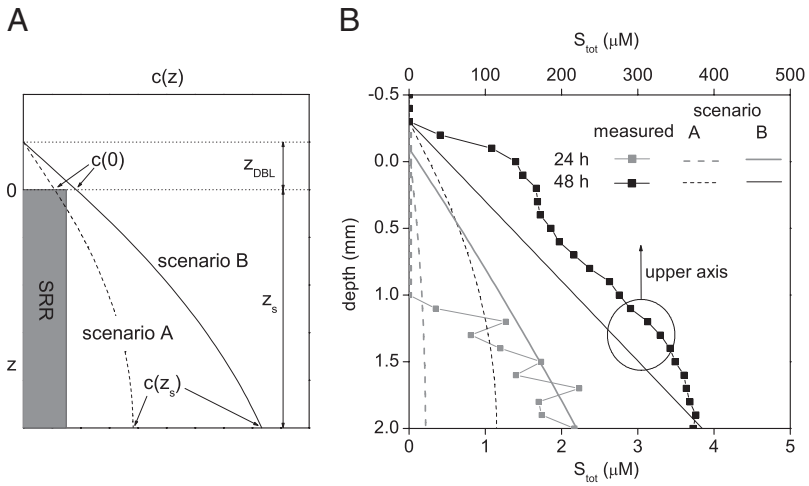

Fig. 4. (*A*) The steady-state diffusive profiles of total sulfide (S_{tot}) concentrations in the sediment covering the coral, modeled based on Eq. 2 in *SI Appendix*, Table S6. S_{tot} produced exclusively in the sediment by sulfate reduction is shown by the dashed line, whereas S_{tot} additionally produced at the coral surface by decomposing coral tissue is shown by the solid line. (*B*) Measured (squares) and the matching modeled (solid lines) profiles of S_{tot} after exposure times of 24 and 48 h. The areal sedimentary sulfate reduction rates (SRR_a) and the total sulfide flux due to coral tissue decomposition (J_d) used to calculate the profiles are listed in Table 1, scenario B. For comparison, dashed lines show S_{tot} profiles calculated by considering the same SRR_a but no coral tissue decomposition (Table 1, scenario A). 0, sediment surface; z, depth; z_s, sediment layer thickness; z_{DBL}, diffusive boundary layer thickness; c(z), S_{tot} concentration at depth z; $c(z_s)$, S_{tot} concentration at the bottom of the sediment layer.

to the input of organics and also decompose polymers under anoxic conditions (32). The high respiration rates in these sediments and the probable resulting fermentation of coral excretions lead to anoxia and low pH, the combination of conditions that leads to coral death. The C_{org} concentrations of the sediments used in this study [increasing natural untreated sediments from 1.25% dry weight (DW) C_{org} by +0.06, +0.3, and +0.6% C_{org} and using natural plankton as source of C_{org}] were conservative and environmentally relevant. For example, the difference in C_{org} concentrations in inshore and offshore silt sediments can be over twofold (1.8 vs. 0.8%) (3). New nutrients from terrestrial runoff are incorporated rapidly into microbial and plankton food webs, leading to increased production and biomass (33). Through the formation of marine snow, aggregates of plankton and muddy sediments with high C_{org} settle on the seafloor and on benthic organisms (17). Hence, it is important for coastal management to understand that it is not sedimentation per se but rather the enrichment of coastal areas with organic matter that can be strongly detrimental for coral survival on inshore coral reefs. Our data show that even relatively small increases (0.3 and 0.6%) in the concentrations of organic matter can lead to rapid onset of photophysiological stress [conventionally measured as quantum yield of the photosystem II of the corals' zooxanthellae (34)] and to reduced survival of corals exposed to sedimentation.

The microbial mechanisms with causal links to biogeochemical processes turned out to be more complex than anticipated. Our hypothesis that H_2S originating from sedimentary sulfate reduction was the cause for the mortality of sediment-covered coral surfaces was not correct. H_2S was not needed for initiating coral death, because low pH alone kills corals during anoxia. The cause of coral death was confirmed in experiment 3, which showed that corals died in anoxic seawater at pH 7.0 (without H_2S) within 24 h. H_2S was not tested separately (e.g., at anoxia, pH 8.2) because (*i*) these conditions never were measured by microsensors during experiment 1, and (*ii*) the dissociation of the sulfur species is pH dependent, so that we would have tested

Table 2. Photosynthetic yields of the coral *Montipora peltiformis* measured by PAM when exposed to darkness, anoxia, reduced pH, and subsequently to H_2S

Exposure parameters	Control	Dark, pH 8.2	Dark, pH 7	12 h anoxia pH 7, then 3 h H_2S	12 h anoxia pH 7, then 12 h H_2S
Light	12 h	No	No	No	No
pH	8.2	8.2	7	7	7
O_2 [μM]	207	207	207	0	0
H_2S [μM]	0	0	0	20	20
Exposure [h]	Yield (SD)	Yield (SD)	Yield (SD)	Yield (SD)	Yield (SD)
0	0.496 (0.017)	0.456 (0.037)	0.463 (0.023)	0.510 (0.049)	0.480 (0.045)
3	0.503 (0.049)	0.467 (0.040)	0.505 (0.022)	**0.063** (0.059)	—
6	0.495 (0.047)	0.453 (0.033)	0.478 (0.028)	—	—
12	0.471 (0.028)	0.446 (0.034)	0.458 (0.021)	—	**0.069** (0.069)
24	0.489 (0.031)	0.467 (0.028)	0.491 (0.033)	—	—
48	0.479 (0.013)	0.452 (0.034)	0.471 (0.027)	—	—
72	0.456 (0.014)	0.462 (0.033)	0.451 (0.024)	—	—
96	0.504 (0.009)	0.458 (0.030)	0.445 (0.023)	—	—
Recovery (48 h)	0.492 (0.006)	0.443 (0.029)	0.478 (0.025)	0.068 (0.055)	0.081 (0.132)

Photophysiological stress of the coral was measured at the indicated exposure time (h) and after 48 h of recovery. Bold numbers indicate the yield at the exposure time after which the coral did not survive the treatment. SDs are based on n = 3–5. For the statistical analysis, see *SI Appendix*, Table S7.

Table 3. Photosynthetic yields of the coral *Montipora peltiformis* measured by PAM when exposed to darkness, anoxia, and reduced pH

Exposure parameters	Anoxia pH 8.2	Recovery (48 h)	Anoxia pH 7	Recovery (48 h)
Light	No	Yes	No	Yes
pH	8.2	8.2	7	8.2
O_2 [μM]	0	207	0	207
H_2S [μM]	0	0	0	0
Exposure [h]	Yield (SD)	Yield (SD)	Yield (SD)	Yield (SD)
0	0.474 (0.016)	—	0.474 (0.016)	—
6	N.a.	—	0.323 (0.066)	0.504 (0.019)
12	N.a.	—	0.227 (0.064)	0.501 (0.021)
25	0.448 (0.043)	0.488 (0.033)	**0.178** (0.120)	**0.154** (0.108)
48	0.453 (0.027)	0.460 (0.027)	0.068 (0.048)	0.069 (0.049)
72	0.486 (0.024)	0.466 (0.030)	0.092 (0.071)	0.117 (0.107)
96	0.476 (0.034)	0.455 (0.028)	0.061 (0.050)	0.111 (0.132)

Photophysiological stress of the coral was measured at the indicated exposure time (h) and after 48 h of recovery. Bold numbers indicate the yield at the exposure time after which the coral did not survive the treatment. SDs are based on n = 3–5. For the statistical analysis, see *SI Appendix*, Table S7.

mainly the exposure to hydrogen sulfide ions (HS^-) instead of to H_2S (see also the explanation below). However, testing the exposure of H_2S at pH 8.2 cannot be considered crucial for this study, because small, discrete spots of coral tissue (a few square millimeters in size; see Figs. 1 and 2) had died before H_2S was measured. More evidence was revealed in experiment 2, which showed that the SRRs in the sediment layer on the coral were too low to generate the measured H_2S concentrations—and were too low to kill the coral. Therefore H_2S could be excluded as the initial trigger for tissue death. However, H_2S played an important role in accelerating the spread of tissue mortality after small areas of coral tissue had died, as seen in the steep increase of H_2S concentration measured by microsensors. Most of the observed H_2S therefore originated from microbially degraded coral tissue and coral mucus, both known to contain substantial amounts of organic sulfur compounds (35, 36). We postulate that the rapid degradation of the mucus and tissue increased the local H_2S concentrations at the coral surface (Fig. 3). The concentration of H_2S in the sediment layer on the coral increased as the result of continuously decreasing pH, because the S_{tot} equilibrium, consisting of H_2S, HS^-, and sulfide (S^{2-}), depends on the pH (37). H_2S is known to penetrate tissues easily (38) and thus is more poisonous than HS^- or S^{2-}. Therefore H_2S was a further stress factor for the cells of the holobiont surrounding the degraded areas and was assumed to speed up the spread of tissue degradation substantially. In experiment 3, the negative effect on the coral was enhanced when the coral first was exposed to anoxia at pH 7.0 for 12 h and then also to H_2S for 3 h. Thus, the tolerance of the coral holobiont against H_2S might have been lowered by previous anoxia and low pH exposure. Other products from proteolytic processes, such as biogenic amines, phenolic compounds, or ammonia, might have contributed further to the stress during sediment coverage and accelerated mortality.

Degradation of the plankton mixture in the sediment led to an accumulation of acidic end products and decreased the pH in the sediment. Neither anoxia nor pH below 8.1 was detected in the sediment not enriched with the plankton mixture. The mucus of the coral alone apparently was insufficient to induce the degradation processes observed in the enriched sediments. Coral mucus might have biocidal properties, and the SRR of sediment covering live coral was only 25% of that of identical sediment that was not in contact with corals. Thus, corals may suppress sulfate reduction, as also shown by Werner et al. (39).

Surprisingly, O_2 depletion at the coral's surface did not lead to coral damage within 4 d. Also, light exclusion by sediments that were low in organic matter did not affect the photosynthetic yields of the corals' zooxanthellae substantially within 6 d. Thus, anoxia and light exclusion did not have a negative impact on the holobiont. Corals regularly experience hypoxia at night (40) and survive anoxia for several days (41), possibly using fermentation, as shown for other cnidarians (42, 43). However, fermentation can lead to pronounced intracellular acidification (44), eventu-

Table 4. Photosynthetic yields of the coral *Montipora peltiformis* measured by PAM when exposed to darkness, anoxia, reduced pH, and H_2S

Exposure parameters	Anoxia pH 7, 10 μM H_2S	Recovery (48 h)	Anoxia pH 7, 20 μM H_2S	Recovery (48 h)
Light	No	Yes	No	Yes
pH	7	8.2	7	8.2
O_2 [μM]	0	207	0	207
H_2S [μM]	10	0	20	0
Exposure [h]	Yield (SD)	Yield (SD)	Yield (SD)	Yield (SD)
0	0.510 (0.037)	—	0.501 (0.020)	—
6	0.313 (0.046)	0.434 (0.027)	0.050 (0.032)	0.494 (0.051)
12	0.217 (0.080)	0.520 (0.064)	0.055 (0.059)	0.525 (0.098)
24	**0.292** (0.050)	**0.267** (0.169)	**0.055** (0.065)	**0.106** (0.077)
48	0.062 (0.058)	0.135 (0.091)	0.050 (0.028)	0.068 (0.046)

Photophysiological stress of the coral was measured at the indicated exposure time (h) and after 48 h of recovery. Bold numbers indicate the yield at the exposure time after which the coral did not survive the treatment. SDs are based on n = 3–5. For the statistical analysis, see *SI Appendix*, Table S7.

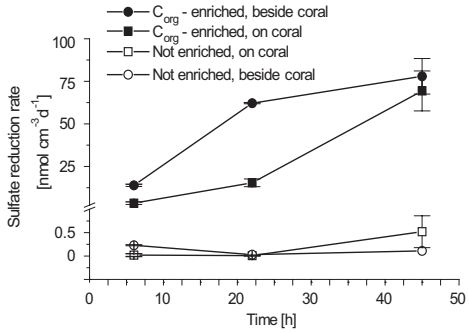

Fig. 5. The SRRs in sediments covering the corals and in controls without coral, determined after exposure times of 6, 22, and 45 h. In this mesocosm experiment one of the sediments was enriched with plankton mixture (+0.6% C_{org}), and the other sediment was not enriched (+0% C_{org}). Error bars represent the SD (n = 2).

ally causing severe cell damage (45, 46) to the animal and its symbionts. It also is possible that the energy costs of maintaining cell pH over longer periods exceed the energy yield from fermentation alone, and the pH-regulation mechanism of one or both organisms of the holobiont eventually breaks down. We suggest that this breakdown is the most likely explanation of the strong effect of lowered pH during anoxia. However, the sediment also may hinder diffusional exchange of anaerobic metabolic products such as succinate, fumarate, and lactate. These products might be more harmful at pH 7.0 than at pH 8.2, because protonated compounds enter cells easier than ions.

The rapid degradation of coral tissue under the sediment might be an infection process. Bacteria normally associated with corals might flourish because of the exposure to organic matter, leading to infections, as shown by Kline et al. (18). However, experiment 3, in which neither sediment nor organic matter was used, revealed that exposing corals to anoxia and pH 7 was sufficient to induce irreversible damage. Still, it might be argued that these conditions favor pathogenic bacteria or trigger bacteria normally associated with corals to become virulent. This argument is weakened by our molecular analysis of the sediments on the coral and in Petri dishes, which revealed similar communities based on the DGGE band pattern. Additionally the curved O_2 and pH microsensor profiles showed increased microbial activities in the organic-rich sediment layers and not at the tissue surface. Taken together, these results suggest that the bacteria associated with the organically enriched sediments flourished, but the coral-associated bacteria did not. Furthermore, we observed that the sediments covering the corals became colonized by white, sulfur-oxidizing bacteria (Fig. 1) (3). Such bacterial communities typically are associated with coral diseases (47) and are a sign of the presence of sulfide. Obviously, these opportunistic bacteria might reduce the sulfide levels. Most likely, sulfide oxidation does not play a role in our scenario for the coral demise, although the acidification associated with this process may be important. The conjunct activity of different microbial groups in organically enriched sediment appears to cause tissue degradation in corals by creating anoxia and reducing pH.

We conclude that sedimentation kills corals through consecutive microbial processes triggered by the presence of organic matter in the sediments. Respiration activities result in anoxia and reduced pH, initiating tissue degradation. Subsequently formed H_2S, released by microbial desulfurylation of coral tissue and mucus, diffuses to and accelerates the degradation of the neighboring tissues. Our data show that the level of organic enrichment of coastal sediments is a key in understanding the degradation of coral reefs exposed to coastal runoff and sediment resuspension.

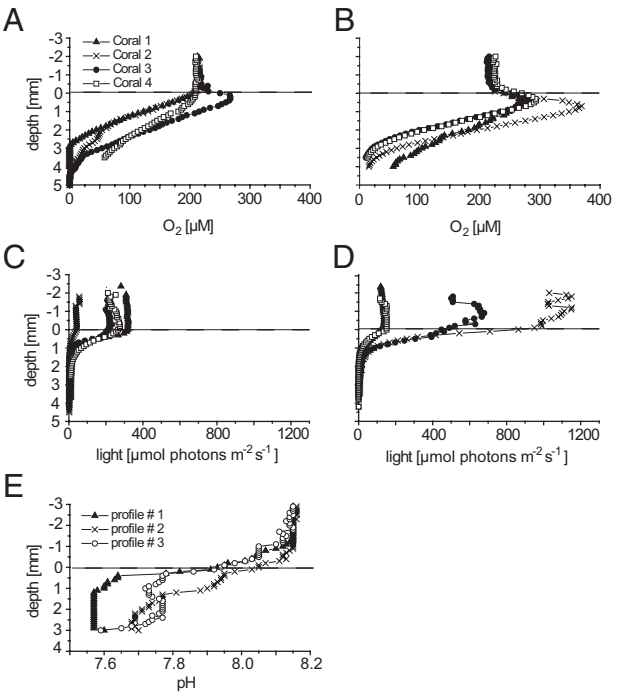

Fig. 6. Microsensor profiles of O_2 (*A* and *B*), light (*C* and *D*), and pH (*E*) at randomly chosen points in natural sediment layers covering corals in the field. O_2 and light profiles were measured on four corals each at nearshore (*A* and *C*) and offshore (*B* and *D*) reefs. (*E*) One coral was chosen for pH profiles at a nearshore reef site. Error bars are omitted for clarity. Each profile represents the average of three profiles measured at randomly chosen points.

Materials and Methods

Coral and Sediment Collection. The flat-foliose coral *M. peltiformis* is an abundant species on nearshore reefs of the Great Barrier Reef of Australia. For the laboratory experiments, coral fragments were collected from Hannah Island (13°52′ S, 143°43′ E) from a water depth of 4–5 m. Fragments of 5–15 cm^2 were kept in flowthrough aquaria under natural light for 2–3 mo or at least until they resumed growth (about 2 wk) before they were used for the experiments. For the field measurements *M. peltiformis*, *Montipora* sp., *Pachyseris* sp., *Porites* sp., and *Turbinaria reniformis* were chosen because they often were observed to be covered by naturally accumulated sediment.

Sediments were collected from the upper 5 cm of sediment deposits at a water depth of 5–10 m on the fringing reef of Wilkie Island (13°46′ S, 143° 38′ E). After collection the sediment was well homogenized and wet-sieved with plastic sieves to obtain the silt-sized fraction of <63 μm, which is found to accumulate most commonly on corals or sampled on reefs in sediment traps (48, 49). The listed properties of the sieved sediment were determined following the methods described by Weber et al. (3): grain size distribution, settling volume, settling rate, compaction, organic matter (ash-free DW), TOC (denoted as C_{org}), TN, TP, Chl *a*, and Phaeo, and 15 elements including the aluminum:calcium ratio. The data are shown in *SI Appendix*, Table S2.

Sediments with different concentrations of labile organic matter but otherwise identical properties were prepared as follows. Plankton, including attached bacteria (14), was collected with a 100-μm net, minced with a blender, sieved to remove large fragments, and frozen. The natural untreated sediment with 12.5 ± 1 μg $C_{org}{\cdot}mg^{-1}$ DW (1.25% C_{org} of sediment DW) was enriched with the plankton mixture, resulting in an additional organic carbon content of +0, +0.06, +0.3, or +0.6% C_{org} (experiment 1) and +0 or +0.6% C_{org} (experiment 2). These sediments were incubated at ambient seawater temperature (24–25 °C) for 24 h in 2 L seawater on a rotor shaker. This procedure was chosen to mimic the runoff event when nutrients and sediment particles are washed into the nearshore reefs, which is explained as follows. During the runoff event microbes and phytoplankton flourish (14, 15, 33) and, together with organic substances and mineral particles, form larger aggregates, called "marine snow" (13), which become heavy enough to sink to the bottom (12). This marine snow has an active microbial community traveling along with the aggregates (14, 15, 30, 31) and eventually ending up on the coral (16). Concentrations of TOC, TN, TP, Chl *a*, and Phaeo were measured in duplicate

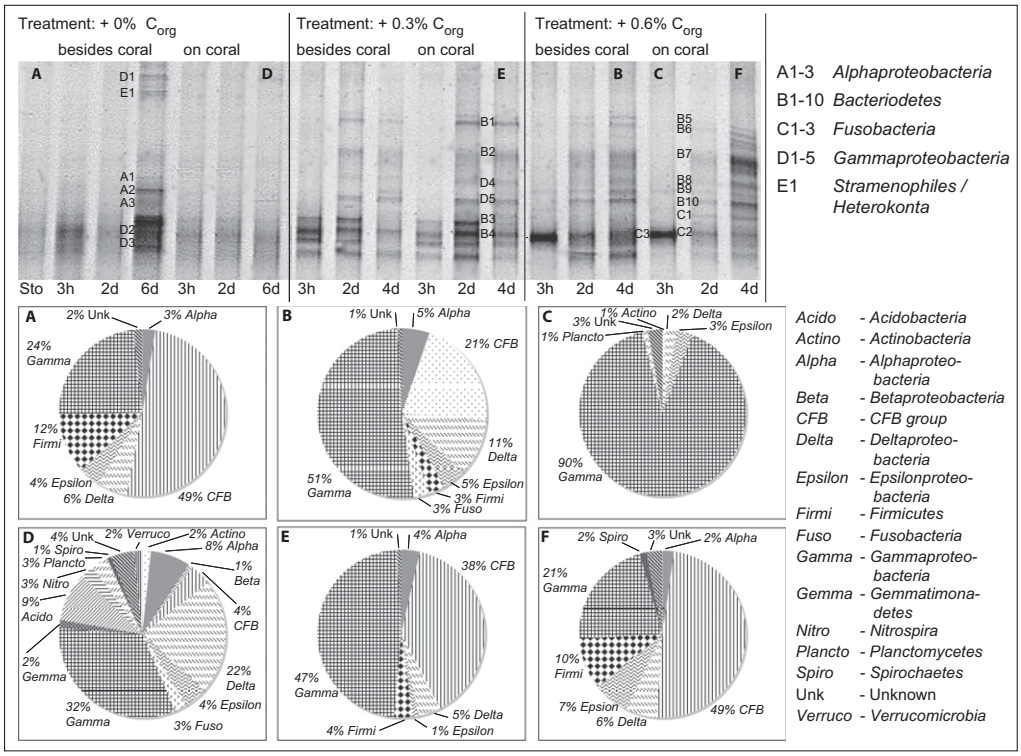

Fig. 7. Analysis of the microbial community of the experimental sediment covers on corals and the control sediments by denaturing gradient gel electrophoresis (DGGE) fingerprints (*Top*) and clone libraries (*Middle* and *Bottom*) after 3 h or after 2, 4, or 6 d. Sto, stock sediment before the start of experiment 1. Sequenced bands are identified in the legend. (*A–F*) Samples used for 16S rRNA clone libraries, displayed also in pie charts. Percentage share refers to the total number of clones obtained in each library (about 120 clones per library; see also *SI Appendix*, Table S5).

subsamples of the sediments and of the plankton mixture. Sediment and plankton characteristics are shown in *SI Appendix*, Table S2).

Experiment 1: Sediment Exposure in Mesocosms. In experiment 1 we quantified the photophysiological stress and area of degraded tissue of *M. peltiformis* in response to exposure to sediment with and without organic enrichment. The measurements were done in outdoor flowthrough mesocosms at the aquarium facilities of the Australian Institute of Marine Sciences in Townsville, Queensland, Australia. Ten coral fragments and 10 Petri dishes (to collect control sediment) were placed in each of eight 60-L tanks (two per treatment) with constant flowthrough of 2 L·min^{-1} seawater at 24–25 °C. Maximum illumination by natural light was 400 μmol photons·m^{-2}·s^{-1}. After the flow was turned off, the amount of sediment necessary to obtain 66 mg DW·cm^{-2} sedimentation was suspended in each tank. The sediment load was chosen based on Weber et al. (3), forming a layer 2.1- to 2.6-mm thick. After the flow was turned on again 2 h later, two more coral fragments (also held for 2 h with no flow) were added to each tank as controls that remained free of sediment. Four randomly chosen coral fragments (two from each tank) and four Petri dishes with sediment were removed after 3 h and after 1, 2, 3, and 4 or 6 d for quantifying the coral stress response and for sediment analysis.

The quantum yield of the photosystem II of the corals' zooxanthellae, taken as a measure of the photophysiological stress status of the coral, was measured using a PAM chlorophyll fluorometer (50) as described by Philipp and Fabricius (4). From each coral fragment, 10–15 PAM readings were taken after 60 min of dark adaptation. PAM measurements were taken before sediment exposure and then at each sampling time on both control corals and treated corals after removal of sediment. Samples of sediment from the corals and of control sediment were collected for microbial community and geochemical analyses as described below. The coral fragments were photographed before and after sediment removal, and the proportion of degraded tissue in the sediment-exposed area was determined photogrammetrically using ImageJ (http://rsb.info.nih.gov/ij/). After the experiments, the control corals were frozen in liquid nitrogen. For further analysis, the coral samples were thawed, the tissue was airbrushed off the skeleton with 60–100 mL filtered seawater, washed three times, freeze-dried, and ground. Total carbon (TC), TN, and total sulfur (TS) of the coral tissue were measured by combustion with a carbon, nitrogen, and sulfur analyzer (NA 1500 Series 2; Fisons Instruments) (*SI Appendix*, Table S2).

Laboratory Microsensor Measurements. At each sampling time microsensor measurements were conducted in the sediment layers of two coral fragments per treatment (one per tank). O_2, H_2S, pH, and light microsensors were prepared as described previously (51–54). The pH sensors were modified for field measurements as described by Weber et al. (55). All microsensors had a tip diameter of 10–30 μm and a stirring sensitivity of <1.5%. The O_2 microsensors were calibrated using air- (20.9% O_2) and nitrogen-flushed (0% O_2) seawater at in situ temperature and salinity. The H_2S microsensor was calibrated by adding 100-μL increments of a 500-mM sulfide (Na_2S) stock solution to a nitrogen-flushed 200-mM phosphate buffer (pH 7.5) at in situ temperature. Subsamples from the calibration solution were fixed immediately in 2% (wt/wt) zinc acetate, and the S_{tot} concentration was determined spectrophotometrically with the methylene blue method (56). The H_2S concentration in the calibration buffer was calculated using the dissociation constant pK_1 of 6.9, determined as described by Weber (57). The S_{tot} in the sediment layer on the coral was calculated from the H_2S and pH profile (58) and the pK_1 of 6.6, corrected for temperature and salinity (59). The pH microsensors were calibrated using standard buffers with pH 7.02 and 9.21 (Mettler Toledo) at in situ temperature. The light microsensor was calibrated against a LI-250 lightmeter (LI-COR).

Vertical profiles of O_2, H_2S, and pH in the sediment layer covering the coral were measured after the coral was transferred into a 12.5 × 7.5 cm flow chamber. The flow conditions were similar to those in the experimental tanks. The microsensors were mounted on a motorized micromanipulator (Faulhaber Group and MM33 from Märzhäuser) and connected to amplifiers. The signals were transferred to a computer using a data acquisition card (DAQ-16XA-50; National Instruments). The microsensors first were moved carefully through the sediment layer until reaching the skeleton. Using a computer-controlled motorized system (software m-Profiler; www.microsen-wiki.net), the microprofiles then were measured upwards in 100-μm steps. On each coral three light profiles were measured at different spots at incident light intensity of 370 μmol photons·m^{-2}·s^{-1} provided by a KL 1500 electronic Schott lamp (Zeiss). O_2 and H_2S and pH profiles were measured only in the dark.

Field Microsensor Measurements. Field microsensor measurements were conducted on four corals per site (two per reef). The two sites were nearshore reefs exposed to river floods (High Island, 17°09′ S, 146°00′ E; Bedarra Island,

17°96′ S, 146°09′ E) and offshore reefs that are not reached by floods (Gilbey Reef 17°34′ S, 146°34′ E; Wardle Reef, 17°27′, 146°32′ E). On each coral, three O_2 and light microsensor profiles were measured at randomly chosen spots in the naturally accumulated sediments with a diver-operated underwater microsensor system (55). Additionally, pH profiles also were measured at High Island. Measurements were conducted at a water depth of 4–5 m during the day at natural illumination (mean: 486 ±116 μmol photons·m^{-2}·s^{-1}; measured by light-loggers from Odyssey Dataflow Systems). Sediment samples were collected for geochemical analyses.

The field microsensors measurements were limited by weather conditions and because sediment on only one coral could be measured per dive. Therefore, we focused on the main parameter, O_2, and when anoxia was detected, we also measured pH.

Molecular Analyses. The structure of the bacterial communities was determined in the +0%, +0.3%, and +0.6% C_{org}-enriched sediment covering the corals and in control sediments (mesocosm experiment 1). Nineteen samples were chosen for DGGE DNA fingerprinting. From those samples, six then were analyzed, constructing 16S rRNA clone libraries. The nucleic acid extraction, PCR (750–800 bp), DGGE (300–550 bp), phylogenetic analysis, and calculation of diversity and richness indices (log e) from the obtained sequences were conducted as previously described (60, 61). The PCR for the DGGE samples and for the excised bands was done with 10 ng DNA using the primers GM5F (with GC clamp) and 970RM. For subsequent sequencing of the bands we used the primers GM5F (with GC clamp) at 58 °C, GM1F, and 907RM at 56 °C annealing temperature, respectively (62). The obtained partial sequences were transformed to consensus sequences using the Sequencher DNA sequence assembly software (http://www.genecodes.com/).

Experiment 2: SRRs and Modeling of S_{tot} Profiles. In experiment 2 we tested whether the SRR in sediments covering the corals increased upon enrichment with the plankton mixture. The measured SRRs then were used in a model to test whether the measured H_2S concentrations could have been derived from the sulfate reduction in the sediment covering the coral or from decaying coral mucus and tissue.

Using a closed water circuit, one coral fragment (5–10 cm^2) was placed in each of six separate beakers (diameter 10 cm, volume 500 mL) at 35–36 permille (ppt) salinity, 26–27 °C, and 450 μmol photons·m^{-2}·s^{-1} illumination for 12 h daily. Water movement was obtained by leading a water-saturated airflow over the water surface of each beaker. The air was led through a washing bottle for saturation, so that the evaporation of the water in the beaker by the airflow was minimized. The reef sediment was enriched with +0.6% C_{org} from the plankton mixture and preincubated for 24 h. Radiolabeled $^{35}SO_4^{2-}$ (Amersham) was added to the seawater to a final activity of 25 kBq·mL^{-1}. Then the sediment was suspended in the beaker and left to settle onto the coral (66 mg DW·cm^{-2}). After 6, 22, and 45 h sediment from two coral fragments and sediment remaining on the beaker bottoms were fixed separately in 20% zinc acetate solution. To measure the radiolabeled sulfide in reduced inorganic sulfur phases, samples were processed according to Kallmeyer et al. (63) using the cold chromium distillation procedure. Porewater sulfate concentration in the sediment layer was assumed to be the normal seawater concentration of 28 mM (i.e., the sediment had just settled). Porosity of the sediment was determined after 6, 22, and 45 h from the weight loss of a known volume of wet sediment after drying to constant weight at 60 °C.

Modeling was used to identify the source of the measured sulfide. We assumed that the sample was laterally homogeneous and that sulfide transport in the sediment was governed by diffusion. Furthermore, we assumed that the sulfide concentration at the top of the diffusive boundary layer ($z = -z_{DBL}$) (64) was zero, and that the sulfide was produced by two processes: sulfate reduction by sediment-associated bacteria, characterized by a homogeneously distributed SRR over the sediment layer of thickness z_s, and a decaying coral tissue, represented by a flux of S_{tot} at the coral–sediment interface (J_d). Based on these assumptions and boundary conditions, the solution to a steady-state 1D diffusion-reaction differential Eq. 1 is given by Eq. 2 in *SI Appendix*, Table S6. This equation was used to calculate the sulfide concentrations and fluxes at the sediment–water (Eq. 3 a and b) and sediment–coral interfaces (Eq. 3 c and d). To reveal the importance of the process of coral tissue decay, the results of this calculation were compared for two scenarios: without decay (scenario A; $J_d = 0$; dashed line in Fig. 4*A*) and with decay (scenario B; nonzero J_d; solid line in Fig. 4*A*). In both scenarios, the measured SRR was used as the sedimentary SRR.

Experiment 3: Exposure to Anoxia, Lowered pH, and H_2S in Mesocosms. To differentiate among the effects of anoxia, lowered pH, and H_2S exposure on *M. peltiformis*, three to five coral fragments (5–10 cm^2) were exposed to each of the treatments listed in Tables 2–4 at 34–35 ppt salinity and 26–27 °C. We conducted three consecutive experiments to investigate (*i*) the effect of anoxia at normal seawater at pH = 8.2 and of anoxia combined with pH = 7.0; (*ii*) the effect of increased sulfide concentration (10 and 20 μM) and exposure time; and (*iii*) the combined affect of anoxia at pH = 7.0 followed by additional sulfide exposure. Darkness, H_2S concentrations, and pH = 7.0 were chosen based on the microsensor data of experiment 1. Concentrations of O_2 and S_{tot} were measured by titration (65) and spectrophotometrically (56), respectively. The sulfide concentration in the seawater was calculated using the pK_1 of 6.5, corrected for salinity and temperature (59). The pH was measured with a sulfide-tolerant pH sensor (IntLab 412/170; Mettler Toledo). The pH was adjusted by adding drops of concentrated HCl. Very slow stirring prevented stratification and imitated the no-flow conditions corals experience during sediment coverage. The anoxia and sulfide treatments were conducted in a glove box (volume 520 L) flushed with N_2. O_2 and temperature sensors continuously monitored the ambient conditions. The photophysiological stress of the coral was measured with the PAM fluorometry as described above. After the experiment the corals were transferred back into a large tank to observe long-term recovery.

Statistical Methods. All statistical analyses were performed in R (R Development Core Team; http://www.r-project.org/). In experiment 1 differences between lengths of exposure and concentrations of C_{org} were analyzed with generalized linear models, using quasi-Poisson error distribution and link function for the yield and degraded tissue data and Gaussian error distribution for the remaining data. Nonsignificant terms were dropped using backward elimination. Differences in the concentrations of Chl *a*, nutrients, and trace elements in the sediment layer deposited on coral colonies from inshore and offshore regions were modeled using ANOVA models. Generalized linear models were used for the following analyses: (*i*) changes in concentrations of O_2, S_{tot}, H_2S, and pH values in the boundary layer directly above the coral colony based on microsensor measurements; (*ii*) changes in concentrations of TOC, TP, and TN over time depending on the concentration of C_{org}, in the sediment above the coral colony or in the Petri dish (control sediment); (*iii*) in experiment 3, changes in photosynthetic yields in response to exposure to darkness, anoxia (O_2), H_2S concentrations, and pH values (8.02 vs. 7.0).

ACKNOWLEDGMENTS. We thank Craig Humphrey and Tim Cooper [Australian Institute of Marine Science (AIMS)] for laboratory and field assistance; Steven Boyle (AIMS), Raphael Wust (then of James Cook University), and Thomas Max and Astrid Rohwedder (then of Max Planck Institute for Marine Microbiology) for analytical support; all technicians of the Microsensor Department of the Max Planck Institute for Marine Microbiology for providing the microsensors; Claudio Richter (then of Leibniz Center for Tropical Marine Ecology), Dieter Hanelt (then of the Alfred Wegener Institute for Polar and Marine Research), and Kai Bischof (University of Bremen) for kindly lending measuring instruments; the editor and all reviewers for extensive input, which greatly improved this article. M.W. thanks Marian Y. Hu (then of IFM-GEOMAR Leibniz-Institute of Marine Sciences) for helpful discussions. M.W. was supported by a doctoral scholarship from the German Academic Exchange Service and the Max Planck Society.

1. Burke L, Reytar K, Spalding M, Perry A (2011) *Reefs at Risk Revisited* (World Resources Institute, Washington, DC).
2. Howarth R, et al. (2011) Coupled biogeochemical cycles: Eutrophication and hypoxia in temperate estuaries and coastal marine ecosystems. *Front Ecol Environ* 9(1):18–26.
3. Weber M, Lott C, Fabricius KE (2006) Sedimentation stress in a scleractinian coral exposed to terrestrial and marine sediments with contrasting physical, organic and geochemical properties. *JEMBE* 336:18–32.
4. Philipp E, Fabricius K (2003) Photophysiological stress in scleractinian corals in response to short-term sedimentation. *JEMBE* 287:57–78.
5. Goreau TF, Yonge CM (1968) Coral community on muddy sand. *Nature* 217:421–423.
6. Rogers CS (1990) Responses of coral reefs and reef organisms to sedimentation. *MEPS* 62:185–202.
7. Fabricius KE (2005) Effects of terrestrial runoff on the ecology of corals and coral reefs: Review and synthesis. *Mar Pollut Bull* 50:125–146.
8. Peters EC, Pilson MEQ (1985) A comparative study of the effects of sedimentation on symbiotic and asymbiotic colonies of the coral *Astrangia danae*. *JEMBE* 92: 215–230.
9. Vargas-Ángel B, Riegl B, Gilliam D, Dodge RE (2006) An experimental histopathological rating scale of sediment stress in the Caribbean coral *Montastrea cavernosa*. *Proceedings of the 10th International Coral Reef Symposium, Okinawa, Japan. June 28-July 2, 2004,* pp 1168–1173.

10. Sofonia J, Anthony KRN (2008) High-sediment tolerance in the reef coral *Turbinaria mesenterina* from the inner Great Barrier Reef lagoon (Australia). *Estuar Coast Shelf Sci* 78:748–752.
11. Gibbs RJ (1983) Effect of natural organic coatings on the coagulation of particles. *Environ Sci Technol* 17(4):237–240.
12. Ayukai T, Wolanski E (1997) Importance of biologically mediated removal of fine sediments from the Fly River plume, Papua New Guinea. *Estuar Coast Shelf Sci* 44:629–639.
13. Passow U (2002) Transparent exopolymer particles (TEP) in aquatic environments. *Prog Oceanogr* 55:287–333.
14. Kaltenböck E, Herndl GJ (1992) Ecology of amorphous aggregations (marine snow) in the Northern Adriatic Sea. IV. Dissolved nutrients and the autotrophic community associated with marine snow. *MEPS* 87:147–159.
15. Grossart HP, Ploug H (2001) Microbial degradation of organic carbon and nitrogen on diatom aggregates. *Limnol Oceanogr* 46(1):267–277.
16. Fabricius KE, Wolanski E (2000) Rapid smothering of coral reef organisms by muddy marine snow. *Estuar Coast Shelf Sci* 50:115–120.
17. Fabricius KE, Wild C, Wolanski E, Abele D (2003) Effects of transparent exopolymer particles (TEP) and muddy terrigenous sediments on the survival of hard coral recruits. *Estuar Coast Shelf Sci* 57:613–621.
18. Kline DI, Kuntz NM, Breitbart M, Knowlton N, Rohwer F (2006) Role of elevated organic carbon levels and microbial activity in coral mortality. *MEPS* 314:119–125.
19. Hodgson G (1990) Tetracycline reduces sedimentation damage to corals. *Mar Biol* 104: 493–496.
20. Bagarinao T (1992) Sulfide as an environmental factor and toxicant: Tolerance and adaptations in aquatic organisms. *Aquat Toxicol* 24:21–62.
21. Jørgensen BB (1982) Mineralization of organic matter in the sea bed - the role of sulphate reduction. *Nature* 296:643–645.
22. Sorokin YI (1978) Microbial production in the coral-reef community. *Arch Hydrobiol* 83:281–323.
23. Dubinsky Z, Stambler N (1996) Marine pollution and coral reefs. *Glob Change Biol* 2: 511–526.
24. Carlton RG, Richardson LL (1995) Oxygen and sulfide dynamics in a horizontally migrating cyanobacterial mat: Black band disease of corals. *FEMS Microbiol Ecol* 18: 155–162.
25. Richardson LL, et al. (2009) Sulfide, microcystin, and the etiology of black band disease. *Dis Aquat Organ* 87:79–90.
26. Kroon FJ, et al. (2011) River loads of suspended solids, nitrogen, phosphorus and herbicides delivered to the Great Barrier Reef lagoon. *Mar Pollut Bull*, in press.
27. Nemeth RS, Nowlis JS (2001) Monitoring the effects of land development on the near-shore reef environment of St. Thomas, USVI. *Bull Mar Sci* 69(2):759–775.
28. Fabricius KE, Golbuu Y, Victor S (2007) Selective mortality in coastal reef organisms from an acute sedimentation event. *Coral Reefs* 26:69.
29. Santschi PH, et al. (1995) Isotopic evidence for the contemporary origin of high-molecular weight organic matter in oceanic environments. *Geochim Cosmochim Acta* 59(3):625–631.
30. Ohnishi Y, et al. (2004) Microbial decomposition of organic matter derived from phytoplankton cellular compounds in seawater. *Microbes Environ* 19(2):128–136.
31. Harvey H, Tuttle JH, Bell JT (1995) Kinetics of phytoplankton decay during simulated sedimentation: Changes in biochemical composition and microbial activity under oxic and anoxic conditions. *Geochim Cosmochim Acta* 59(16):3367–3377.
32. Jørgensen BB (2006) Bacteria and marine biogeochemistry. *Marine Geochemistry*, eds Schulz HD, Zabel M (Springer Verlag, Berlin), pp 173–208.
33. Furnas M (2003) Catchments and corals: Terrestrial runoff to the Great Barrier Reef. (Australian Institute of Marine Science, CRC Reef Research Centre, Rainforest CRC, Townsville, Australia).
34. Warner ME, Lesser MP, Ralph PJ (2010) Chlorophyll fluorescence in reef building corals. *Chlorophyll a Fluorescence in Aquatic Sciences: Methods and Applications*, eds Suggett DJ, Prášil O, Borowitzka MA (Springer, New York) pp. 209–222.
35. Hill R, Dacey JWH, Krupp DA (1995) Dimethylsulfoniopropionate in reef corals. *Mar. Bull. Mar. Sci.* 57(2):489–494.
36. Brown BE, Bythell JC (2005) Perspectives on mucus secretion in reef corals. *MEPS* 296: 291–309.
37. Kühl M, Steuckart C (2000) Sensors for in situ analysis of sulfide in aquatic systems. *In Situ Monitoring of Aquatic Systems. Chemical Analysis and Speciation*, eds Buffle J, Horvai G (Wiley-VHC, Chichester, UK), pp 121–159.
38. Jacques AG (1936) The kinetics of penetration: XII. Hydrogen sulfide. *J Gen Physiol* 19: 397–418.
39. Werner U, et al. (2006) Spatial patterns of aerobic and anaerobic mineralization rates and oxygen penetration dynamics in coral reef sediments. *Marine Ecology Progressive Series* 309:93–105.
40. Kühl M, Cohen Y, Dalsgaard T, Jørgensen BB, Revsbech NP (1995) Microenvironment and photosynthesis of zooxanthellae in scleractinian corals studied with microsensors for O_2, pH and light. *MEPS* 117:159–172.
41. Yonge C, Yonge MJ, Nicholls AG (1932) Studies on the physiology of corals - VI. The relationship between respiration in corals and the production of oxygen by their zooxanthellae. *Great Barrier Reef Expedition 1928–29 Science Reports* (British Museum of Natural History, London), Vol 1, pp 213–251.
42. Ellington WR (1977) Aerobic and anaerobic degradation of glucose by the estuarine sea anemone, *Diadumene leucolena*. *Comp Biochem Physiol* 58B:173–175.
43. Ellington WR (1980) Some aspects of the metabolism of the sea anemone *Haliplanella luciae* (Verrill) during air exposure and hypoxia. *Mar Biol Lett* 1:255–262.
44. Hochachka PW, Fields J, Mustafa T (1973) Animal life without oxygen: Basic biochemical mechanisms. *Am Zool* 13:543–555.
45. Busa WB (1986) Mechanisms and consequences of pH-mediated cell regulation. *Annu Rev Physiol* 48:389–402.
46. Grieshaber MK, Hardewig I, Kreutzer U, Pörtner H-O (1994) Physiological and metabolic responses to hypoxia in invertebrates. *Rev Physiol Biochem Pharmacol* 125: 43–147.
47. Richardson LL (1996) Horizontal and vertical migration patters of *Phormidium corallyticum* and *Beggiatoa* spp. associated with Black-Band Disease of corals. *Microb Ecol* 32(3):323–335.
48. Bothner MH, Reynolds RL, Casso MA, Storlazzi CD, Field ME (2006) Quantity, composition, and source of sediment collected in sediment traps along the fringing coral reef off Molokai, Hawaii. *Mar Pollut Bull* 52:1034–1047.
49. Brooks G, Devine B, Larson RA, Rood BP (2007) Sedimentary development of Coral Bay, St. John, USVI: A shift from natural to anthropogenic influences. *Caribb J Sci* 43(2):226–243.
50. Schreiber U, Schliwa U, Bilger W (1986) Continuous recording of photochemical and non-photochemical chlorophyll fluorescence quenching with a new type of modulation fluorometer. *Photosynth Res* 10:51–62.
51. Revsbech NP (1989) An oxygen microsensor with a guard cathode. *Limnol Oceanogr* 34:474–478.
52. Lassen C, Jørgensen BB (1994) A fiberoptic irradiance microsensor (cosine collector) - Application for in situ measurements of absorption-coefficients in sediments and microbial mats. *FEMS Microbiol Ecol* 15:321–336.
53. de Beer D, Glud A, Epping E, Kühl M (1997) A fast-responding CO_2 microelectrode for profiling sediments, microbial mats, and biofilms. *Limnol Oceanogr* 42:1590–1600.
54. Kühl M, Steuckart C, Eickert G, Jeroschewski P (1998) A H_2S microsensor for profiling biofilms and sediments: Application in an acidic lake sediment. *Aquat Microb Ecol* 15: 201–209.
55. Weber M, et al. (2007) In situ applications of a new diver-operated motorized microsensor profiler. *Environ Sci Technol* 41:6210–6215.
56. Cline JD (1969) Spectrophotometric determination of hydrogen sulfide in natural waters. *Limnol Oceanogr* 14:454–458.
57. Weber M (2009) How sediment damages corals. PhD thesis (University of Bremen, Germany). pp 157–170.
58. Jeroschewski P, Steuckart C, Kühl M (1996) An amperometric microsensor for the determination of H_2S in aquatic environments. *Anal Chem* 68:4351–4357.
59. Millero FJ, Plese T, Fernandez M (1988) The dissociation of hydrogen sulfide in seawater. *Limnol Oceanogr* 33:269–274.
60. Ludwig W, et al. (1998) Bacterial phylogeny based on comparative sequence analysis. *Electrophoresis* 19:554–568.
61. Abed RMM, Kohls K, de Beer D (2007) Effect of salinity changes on the bacterial diversity, photosynthesis and oxygen consumption of cyanobacterial mats from an intertidal flat of the Arabian Gulf. *Environ Microbiol* 9:1384–1392.
62. Muyzer G, Teske A, Wirsen CO, Jannasch HW (1995) Phylogenetic relationships of Thiomicrospira species and their identification in deep-sea hydrothermal vent samples by denaturing gradient gel electrophoresis of 16S rDNA fragments. *Arch Microbiol* 164:165–172.
63. Kallmeyer J, Ferdelman TG, Weber A, Fossing H, Jørgensen BB (2004) A cold chromium distillation procedure for radiolabeled sulfide applied to sulfate reduction measurements. *Limnol Oceanogr Methods* 2:171–180.
64. Jørgensen BB (2001) Life in the diffusive boundary layer. *The benthic boundary layer*, eds Boudreau PB, Jørgensen BB (Oxford Univ Press, Oxford, UK), pp 348–373.
65. Winkler LW (1888) Die Bestimmung des in Wasser gelösten Sauerstoffs [The determination of oxygen dissolved in water]. *Chemische Berichte* 21:2843–2854.